12

MESOMETEOROLOGY PROJECT

Department of the Geophysical Sciences
The University of Chicago

STUDY OF A LONG CONDENSATION TRAIL PHOTOGRAPHED BY TIROS I

by

Toshimitsu Ushijima

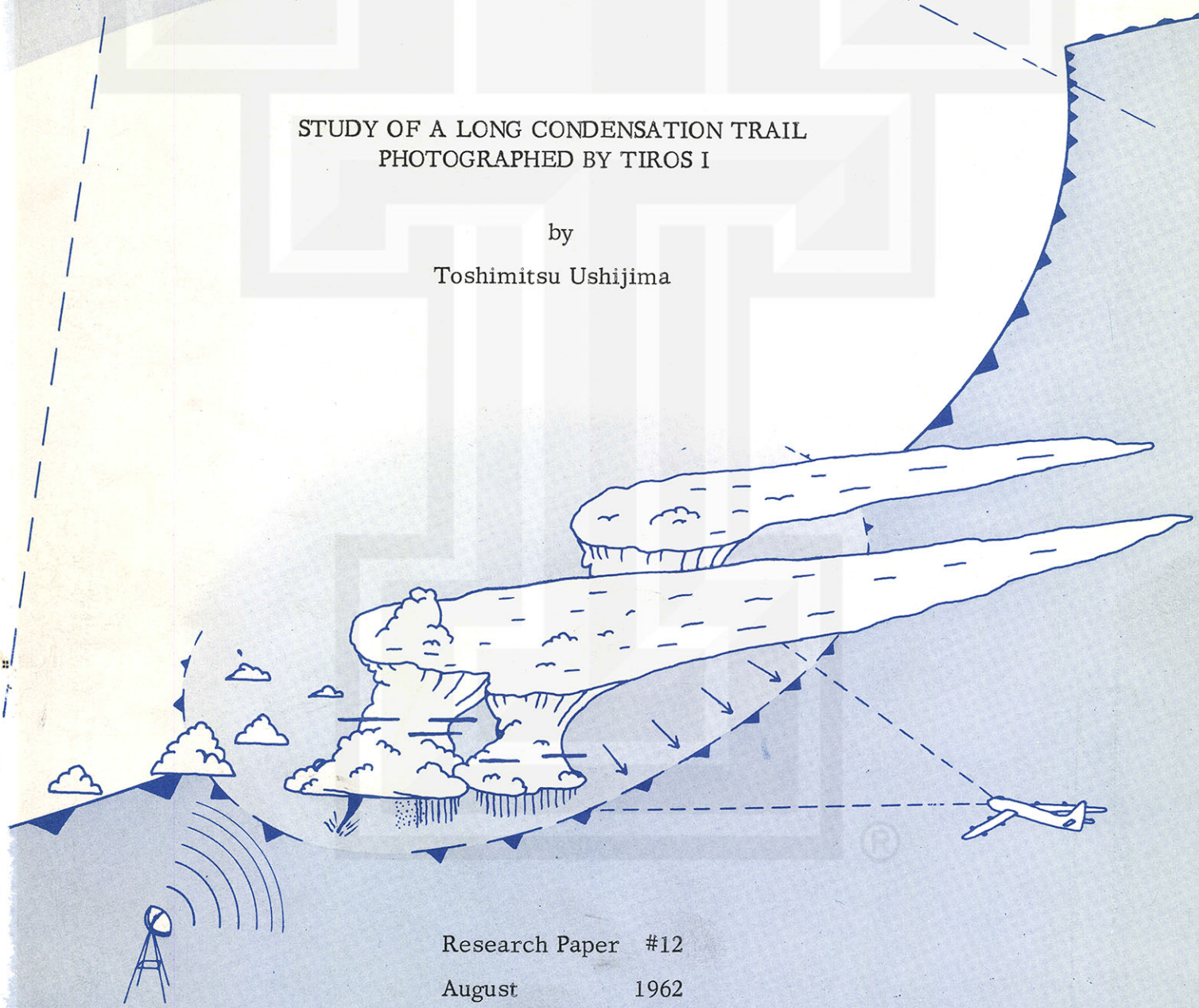

Research Paper #12

August 1962

RESEARCH PAPER # 12

MESOMETEOROLOGICAL PROJECT
Department of the Geophysical Sciences
The University of Chicago

STUDY OF A LONG CONDENSATION TRAIL PHOTOGRAPHED BY TIROS I

by

Toshimitsu Ushijima

The research has been supported by the United States Weather Bureau under contract Cwb 10215 (MSL).

ABSTRACT

A long, thin line of clouds photographed by TIROS I was rectified by the use of a precise technique. As a result of the analysis, it was postulated that the cloud was a long contrail. With reasonable assumptions, probable paths of the aircraft are computed. Wind variation, which caused bends of the line cloud, are also calculated. The two major wavelengths found in the wavy profile of the wind variation are approximately 120 and 20 miles respectively. A method of determining the location of the sun glints is discussed briefly, and a nomogram with which to compute the location of theoretical sun glints is presented.

I. Introduction

Following the successful launching of the TIROS I satellite on April 1, 1960, the value of satellite data to meteorological research and operation was considered by various researchers. Notably, Fritz and Wexler (1960) presented the analytical results of cloud photographs obtained during a period of a few days following the launch. The photographs, taken by a wide-angle camera with a 105 degree field of view, were found to be capable of representing nephsystems in various scales larger than about three miles.

Due to such a high resolution of wide-angle photographs, it is feasible that the cloud patterns of mesoscale disturbances be investigated by using TIROS photographs in combination with the meteorological data. The well known isolated nephsystem of May 19, 1960, appearing on a TIROS I photograph as a square-shaped cloud, was studied by Whitney and Fritz (1961). The case of an isolated but oval-shaped cloud in TIROS photographs was investigated by Blackmer (1961), utilizing radar photographs. He found that operational analysis techniques which were used for rectification were not accurate enough to relate the positions of radar echoes and

clouds. A slight adjustment was made so that echo and cloud areas would correspond.

In order to use satellite photographs in mesometeorological research, Fujita (1961) developed a technique for precise rectification of satellite cloud photographs. With the aid of this technique, which does not involve errors exceeding 0.1 or 0.2 degrees of latitude, both longitude and latitude lines may be drawn directly on cloud photographs.

In the chapter "Planet Earth as Seen from Space", Fritz and Wexler (1961) presented photographs of various nephsystems as viewed from TIROS I. On the photograph taken on August 16, 1960, was a thin, long line of clouds located over the Atlantic, near the southeast coast of the United States. A preliminary investigation of the meteorological conditions existent on that date showed that the area in which the line was located was influenced by a pressure ridge extending from the Bermuda High. Therefore, it seemed unlikely that the line consisted of a row of convective clouds. Also appearing on these photographs were regions of seemingly thin clouds. After a cursory examination it was found that these were actually sun glints. In order to eliminate confusion regarding the interpretation of these seemingly thin clouds, a computational scheme was devised to readily locate the position of sun glints.

II. Preliminary Rectification of Direct-Readout Picture from Orbit 658, TIROS I

From six direct-readout photographs three were selected for rectification. Examination indicated that these three pictures included the entire area of the long, thin nephsystem under question. For purposes of rectification using Fujita's method, the following data were obtained from the Meteorological Satellite Laboratory, U. S. Weather Bureau:

1. Actual Exposure Time
   Frame # 13D (19h 13m 32s GMT), # 16D (191432), # 20D (191532)

2. Orbital Information of Satellite from NASA Attitude Map

Time (GMT)	Latitude	Longitude	Height
19h 10m	24.0N	88.2W	727 km
11	26.4	85.5	729
12	28.9	82.7	731
13	31.2	79.8	732
14	33.5	76.7	734
15	35.6	73.4	736

In general, the method of preliminary rectification consists of plotting the Terrestrial Satellite Subpoints (TSP) at one-minute intervals on an Oblique Equidistant Cylindrical (OEC) projection and determining the appropriate values of longitude on this projection. If the times of the photographs are known, the exact position of the satellite can be plotted on the OEC. In the case of direct-readout photographs, the time of each frame is known within an accuracy of one second. Therefore, it was possible in this case to determine the TSPs from given information rather than from interpolation. In Fig. 1 the TSPs for Frame #13, #16, and #20 are shown as open circles.

After completion of the preliminary rectification, it was found that the relative positions of landmarks on the photographs did not coincide with the positions of these landmarks determined from maps. To make the landmarks coincide a shift of 30 miles along the TSP track was made. The necessity of this shift indicates that the satellite tracking and/or time of exposure of these direct-readout photographs was not accurate. Although the cause of such an appreciable error can only be presumed, the adjustment of the TSPs along their track seemed justified. These adjusted TSPs are shown in Fig. 1 as painted circles.

From the proximity of the TSP track to the TPP track it was found that the minimum nadir angle was extremely small. Actual measurements revealed that it was near zero degrees of arc. Difficulties in the determination of the Terrestrial Spin Axis points (TSAs) are encountered where the minimum nadir angle is very small, as in this case. Moreover, the photographs did not contain many cloud patterns that were photographed more than once, so that the track of principal points of other images

could be plotted easily on a single photograph to determine the TPP track on the single image. Since the plot of the TPPs on a single image should be a smooth curve, a best fit smooth curve was drawn on each image for all the available TPPs. These tracks were then checked for consistency on each photograph. The best approximation to the principal line was then made from the consistent positions of the TPPs on each image. In this manner, it was possible to grid each photograph with latitude and longitude lines, even in the absence of what is normally considered necessary data.

III. Results of Rectification

The three pictures which were gridded with longitude and latitude are shown in Figs. 2, 3, and 4. In view of the accuracy of the rectification, which was found to be in error by no more than 0.2 degrees of arc, both longitude and latitude lines were drawn directly on the photographs at one-degree intervals.

From these gridded photographs cloud patterns were transcribed onto the map as presented in Fig. 5. There were three types of nephsystems in the area of analysis. The first type, which was found over the southeastern United States, was characterized by both high and low clouds. The second one, seen near the southeastern corner of the map, was located near the ridge line of the Bermuda High and appeared on photographs as faint cloud masses. The third was a long, thin nephsystem extending from near Miami to the northeast. The configuration and characteristics of this nephsystem were suggestive of a condensation trail (contrail) produced by a single aircraft or possibly a group of aircraft. Since the contrail extended from near Miami, it was assumed that it was caused by jet aircraft that departed from or returned to Miami.

IV. Weather Situation on May 16, 1960

Figure 6 shows the surface weather situation at approximately the same time as the photographs. The area covered by both Figs. 5 and 6 is identical. There was a topographic trough line along the leeward side of the Appalachian Mountains

and a ridge line along the windward side. Except in the northwestern part of the chart, there were no organized cloud areas because most of the area was under the influence of the Bermuda High. Winds were light in most of the area. In order to represent the situation of the upper winds for 18Z, the time of the surface chart, vector-mean winds were computed from 12Z and 24Z observations. The distribution of vector-mean winds appears in Fig. 7. Also included in this figure are the mean temperatures computed from the 12Z and 24Z reports. Isotachs are drawn for each 10 knots.

As can be seen in the isotach pattern, a narrow zone of relatively low wind exists between the polar jet, near the northeast corner of the map, and the sub-tropical jet. The axis of the sub-tropical jet stream extends from the north coast of the Gulf of Mexico to the southern tip of the Florida peninsula. The winds along these jet axes at the 200-mb level were over 70 knots (polar jet) and 60 knots (sub-tropical jet). In contrast, the zone of low-wind speed indicated only up to 40 knots.

V. Computation of the Drift Distance of the Contrail

As can be seen in Fig. 7, the length of the contrail was approximately 600 miles, and near its southern end there was a break in the line. When measured on the photographs, the width of the line varied along its length from near zero to seven miles. If consideration is given to the resolution of the TIROS photograph, which is assumed to be three miles, the true width of the line could be reduced from the measured seven miles.

It may be argued that a width of about four miles would be too wide for a contrail; however, the trail may have been formed by a fleet of jet aircraft and then diffused during the time between its formation and the time of the photographs. Another possible explanation of this large width of the line is the effect of sun glint. As seen in the photographs, the wide portion of the contrail is located near the area of sun glint. This would suggest that the line was in such a position relative to the satellite that the cloud top reflected the sunbeams most efficiently back into the TIROS camera. This fact would result in the actual width of the contrail being much narrower than

four miles, which was the estimated width without taking the above fact into consideration.

After justifying this line cloud as being a contrail, it is necessary to estimate the direction of the flight path. As seen in Fig. 7, the northeastern end of the contrail is located off the coast of Cape Hatteras and has greater curvature than the other end, which was only 30 miles east of the Florida coast. From these features of the contrail, it was assumed that the aircraft flew from the northeast to the southwest. The following assumptions were then made:

1. Speed of the aircraft was 600 miles per hour.
2. It flew at the 200-mb level.
3. It terminated in the Miami area.

The position where each segment of the contrail originated can be obtained, if the time when the last segment at the southwestern end of the line was produced is known. If we assume that the last segment was produced at 1913Z, the time of the TIROS photographs, the position of the initial contrail can be obtained by shifting the contrail segment upstream. The amount of the shift, ΔS, can be computed by

$$\Delta S = V \Delta t$$

where V denotes wind velocity at the 200-mb level, and Δt at the time difference between 1913Z and the time when the contrail segment was produced. Since it was assumed that the speed of the aircraft was 600 miles per hour, the time difference, Δt, for the contrail segment, P, in Fig. 8 can be written as $60\,\overline{EP}/\overline{BE}$ (in minutes). A computation was made for each significant point along the wavy contrail. The resultant displacements were then connected by the dashed line shown in Fig. 8. As can be seen in this figure, the dashed line of these displacements has most of the characteristics of the rectified cloud line. The wavy dashed line would represent the flight path of the aircraft producing the contrail. It is difficult to comprehend that the jet aircraft which produced the contrail flew along this wavy dashed line. Therefore, it would be more natural to smooth the dashed line in order to represent a reasonable flight path. Thus, the heavy smooth line E_oB_o in the figure was drawn.

There is no reason to believe that the end of the contrail had been produced at

1913Z when the TIROS picture was made. If it were produced one, two, or three hours prior to 1913Z, the flight paths corresponding to these cases would be shifted further to the west-northwest. Under the assumption of a steady state of the 200-mb winds, the flight path B_1E_1, B_2E_2 and B_3E_3 were obtained.

VI. Mesoscale Variation of Wind Velocity

The contrail under discussion was characterized by many kinks and bends. The assumption that the aircraft flew along a rather smooth path leads us to conclude that the kinks and bends resulted from the variation of the horizontal winds at the flight level.

The amount of the variations can be computed against each of these hypothetical flight paths, B_oE_o, B_1E_1, B_2E_2, etc.. Figure 9 represents the profile of the computed variations. If the true variation of wind speed along the flight path is represented by the variation (120 knots per 50 miles) shown in the top diagram (B_oE_o), then, in general, wind forecasts along a particular flight path could not possibly be accurate. Therefore, it is assumed that the top profile is unreasonable. The middle profile (B_1E_1) seems reasonable since the variation about the mean value is approximately 15 knots. The path, B_2E_2, is also acceptable in view of the smaller variation.

It should be noted that the space distribution of the variation is rather regular with the spacial wavelength being about 120 and 20 miles. The wavelength might be much shorter; however, the resolution of the photographs does not permit detection of such wavelengths. These wavelengths represent the characteristic dimensions of mesoscale disturbances which have been analysed on surface maps.

VII. A General Method of Determining the Location of Sun Glints

The dim reflection areas along the coast line in the photographs, appearing in Figs. 2, 3, and 4, are sun glints. An actual reflection of the sun is noted in Fig. 3. These glints are produced by the reflected sunbeams from the ocean surface back to

the TIROS camera. It is known that the glint is extremely bright when reflected from a smooth sea or lake surface. The small brilliant spot seen in Fig. 3 may indicate that an extremely smooth lagoon or inland waterway existed at that position.

The following is a method for determining the location of the sun glint. Let θ be the angle between the TSP and the sun glint; η^*, the object-nadir angle; R, the radius of the Earth; and H, the height of the satellite (see Fig. 10). From the geometry of Fig. 10, it can be shown that

$$R\cos\theta + R\sin\theta\cot\eta^* = R + H \tag{1}$$

Using the relation,

$$\theta = \frac{1}{2}\left(\frac{\pi}{2} - a - \eta^*\right), \tag{2}$$

(1) can be solved as

$$\cos\frac{1}{2}\left(\frac{\pi}{2} - a - \eta^*\right) + \sin\frac{1}{2}\left(\frac{\pi}{2} - a - \eta^*\right)\cot\eta^* = 1 + H/R \tag{3}$$

where a is the altitude of the sun.

Both a and a_s, azimuth of the sun measured eastward from north can be obtained by

$$\sin a = \sin\phi\sin d + \cos\phi\cos d\cos h \tag{4}$$

and

$$\sin a_s = \cos d\sin h/\cos a \tag{5}$$

where ϕ is the latitude of the TSP; d, the declination of the sun; h the hour angle of the sun measured eastward from the TSP as being positive and westward, negative.

A nomogram to calculate the η^*as a function of a and H is shown in Fig. 11. In order to examine the slopes of the isopleths of η^*, we differentiate the satellite height with respect to a, the elevation angle of the sun. Thus,

$$\left(\frac{\partial H}{\partial a}\right) = \frac{R}{2\cos\frac{1}{2}(\frac{1}{2}-a-\eta^*)}\left\{\cot\eta^* - \tan\frac{1}{2}(\frac{\pi}{2}-a-\eta^*)\right\}. \quad (6)$$

This derivative is zero when satisfies the condition,

$$\eta^* = a + \frac{\pi}{2} \quad (7)$$

This condition, when the sunbeams penetrate the apparent horizon and procede directly into the camera of the satellite, shows that the height of the satellite at a constant-nadir angle reaches its maximum value. The line consisting of these critical points is shown by a dash-dotted line in the nomogram.

The process for determining the location of the sun glint is as follows. η^* is to be calculated from a and H, using the nomogram. If the time and the TSP are known, a and a_s can be computed from Equations (4) and (5) or the nomograms given in the Smithsonian Meteorological Tables.

Now that the object-nadir angle and the azimuth angle of the sun glint viewed from a satellite at any moment are known, the exact position of the sun glint can be plotted on an OEC projection map with the aid of the proper height grid.

The above method was utilized in determining the sun glints, G#13, G#16, and G#20 (Fig. 5) which correspond to the TSPs for Frame #13, #16, and #20 respectively. The locations of these sun glints were compared with the corresponding photographs to see how they appear on each frame. It was found that a dim reflection area existed around the computed sun glint point. In Frame #16, however, (Fig. 3) the bright sun glint is vividly portrayed.

VII. Conclusion

Various reasons were presented to explain the long, thin nephsystem photographed by TIROS I as being a large contrail. Using reasonable assumptions, the path of the

aircraft which produced the contrail was estimated. In addition, the wind variation at the level of the contrail was deduced from its kinks and bends. The profile of the wind variation shows that it was characterized by two major wavelengths, which represent characteristic dimensions of mesoscale disturbance. Besides the study of the contrail, a method was developed by which the location of the sun glint can be determined within the limits of rectification.

Due to the sparcity of upper air data, it has been difficult to investigate mesoscale disturbance in the upper troposphere. With increasing knowledge of the physical changes that nephsystems undergo, it is believed that satellite photographs will be the future data from which atmospheric motions can be deduced.

Acknowledgment

The author wishes to thank Dr. Tetsuya Fujita for his kind guidance and comments.

References

Blackmer, R., 1961: Satellite observation of squall line thunderstorms. Proceeding of the Ninth Weather Radar Conference, 76-82.

Fritz, S., and H. Wexler, 1960: Cloud pictures from satellite TIROS I. Mon. Wea. Rev., 88, 79-87.

Fujita, T., 1961: Outline of a technique for precise rectification of satellite cloud photographs. Res. Paper 3, Mesomet. Proj., U. of Chicago.

Whitney, L., and S. Fritz, 1961: A tornado-producing cloud pattern seen from TIROS I. Bull. of A. M. S., 42, 603-604.

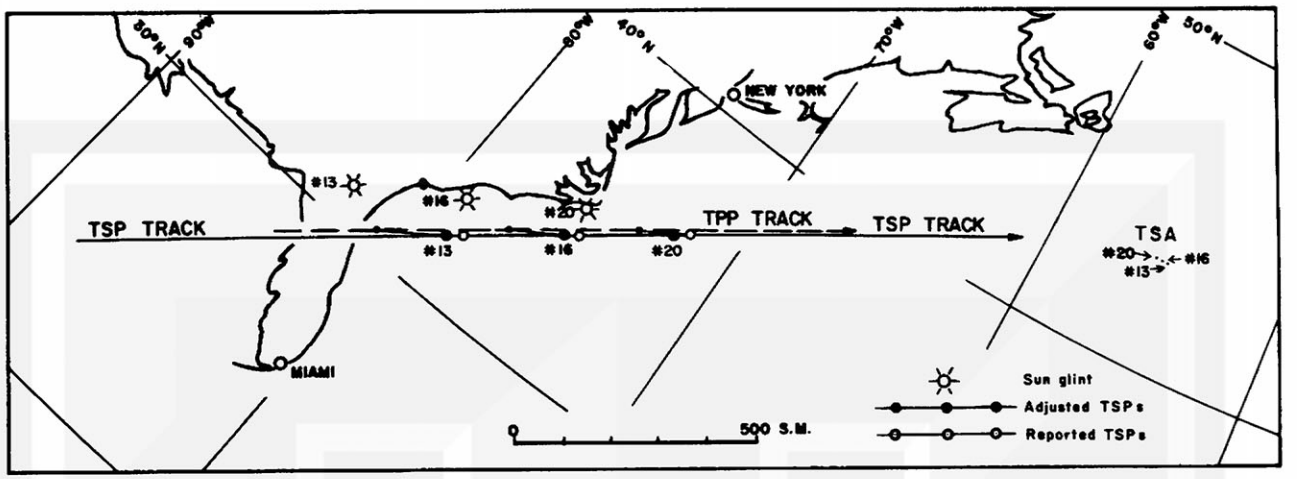

Fig. 1. TPP track, TSP track and TSAs of the orbit 658 on May 16, 1960.

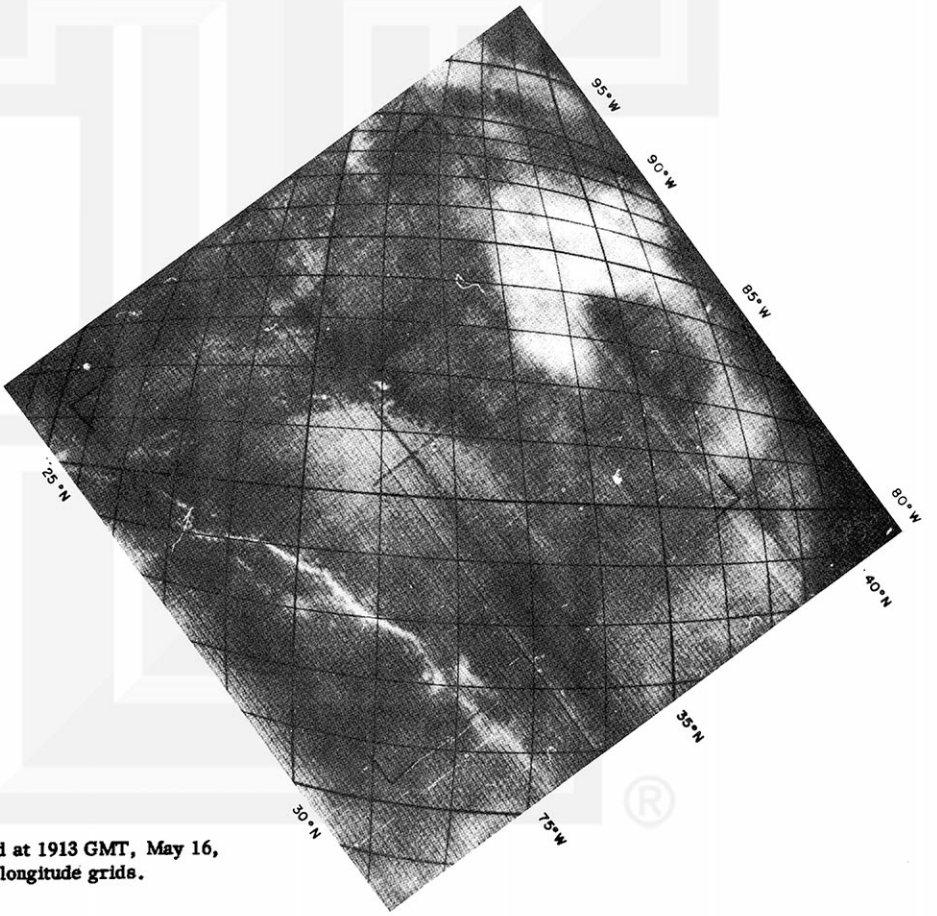

Fig. 2. TIROS I photographed at 1913 GMT, May 16, 1960, with computed latitude and longitude grids.

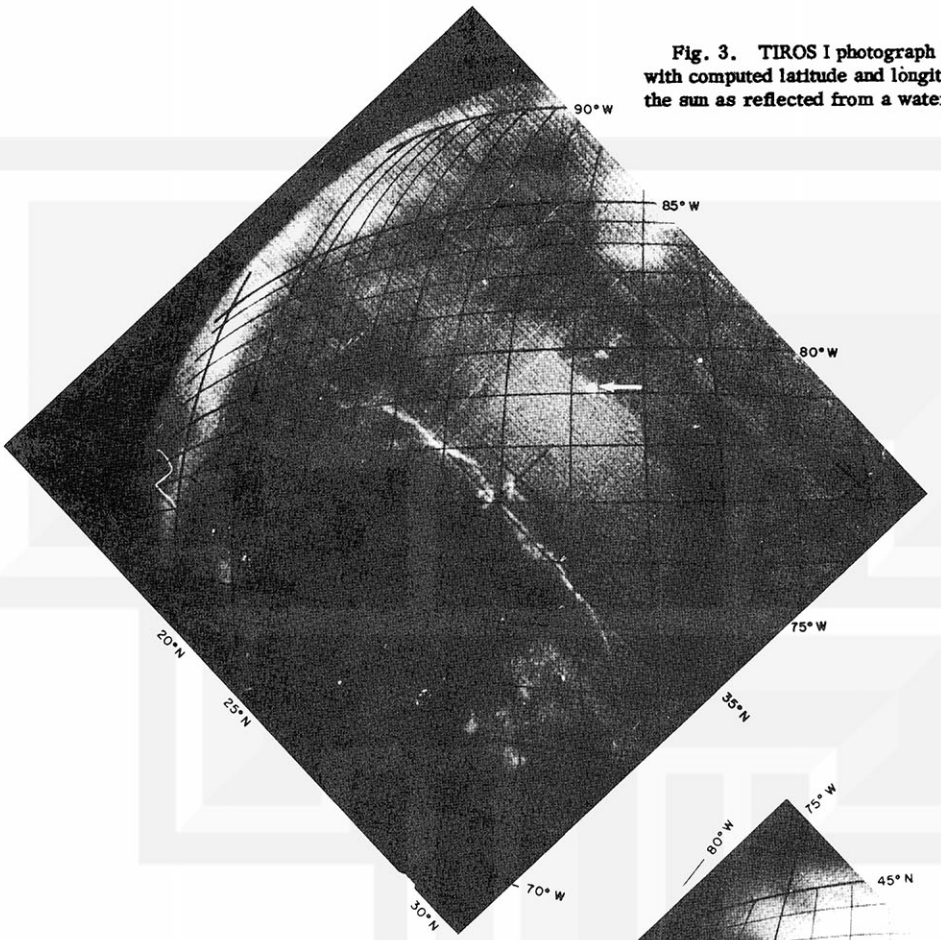

Fig. 3. TIROS I photograph at 1914 GMT, May 16, 1960, with computed latitude and longitude grids. Arrow indicates the sun as reflected from a water surface.

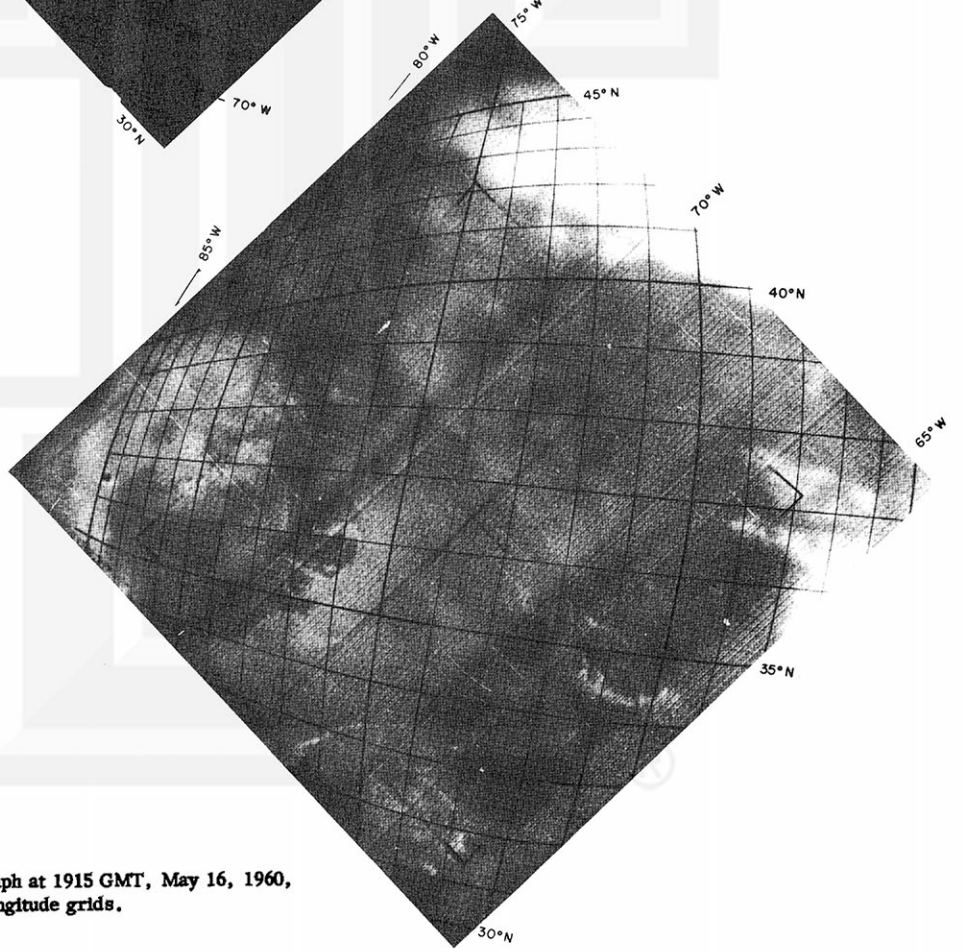

Fig. 4. TIROS I photograph at 1915 GMT, May 16, 1960, with computed latitude and longitude grids.

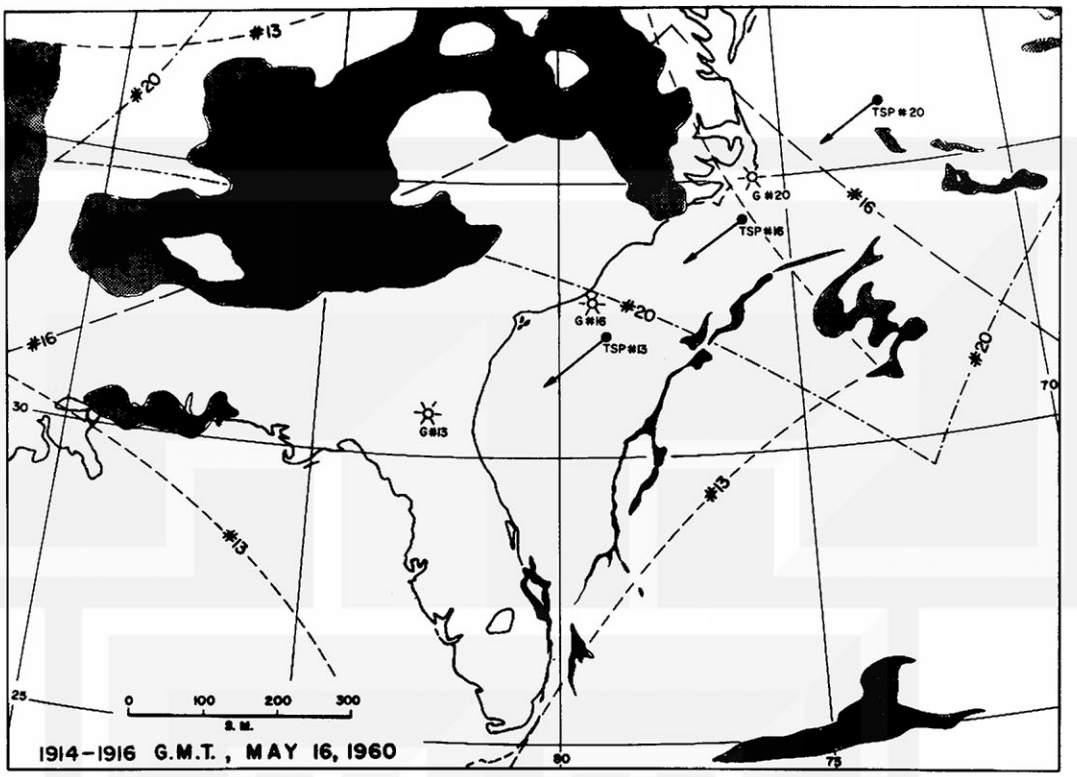

Fig. 5. TIROS photographed clouds as they would appear on the usual Lambert conformal map. Solid areas indicate brightest regions on the photograph.

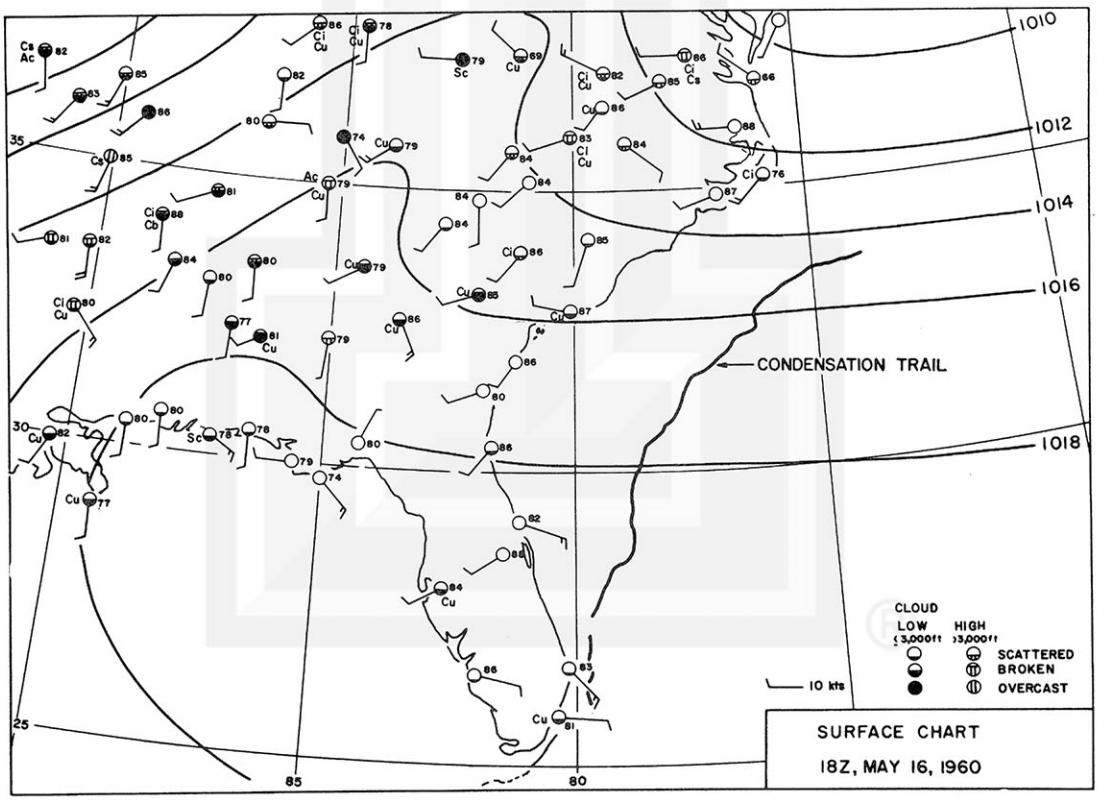

Fig. 6. Chart of measured surface meteorological parameters less than one hour prior to the TIROS photographs. Note the influence of high surface pressure in the region of the condensation trail.

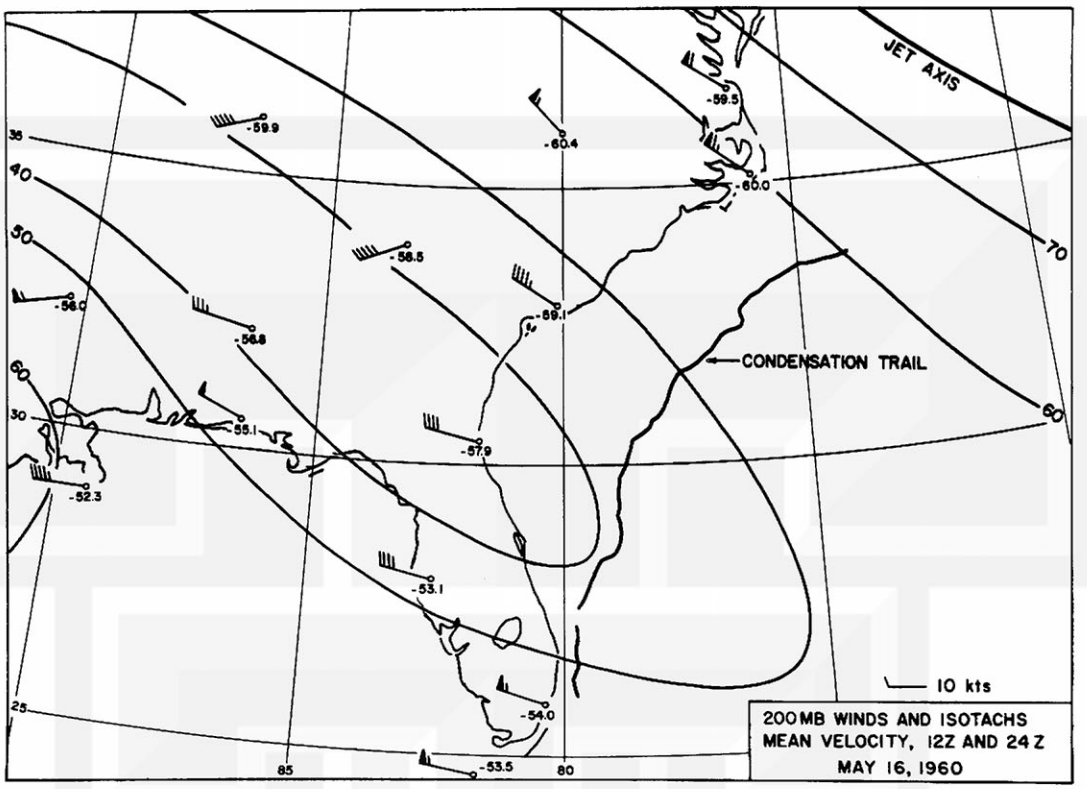

Fig. 7. Spatial distribution of 200-mb average temperature (°C) and average wind velocity for 12Z and 24Z, May 16, 1960. Isotachs are drawn to show the narrow region of minimum speed between the jet axes.

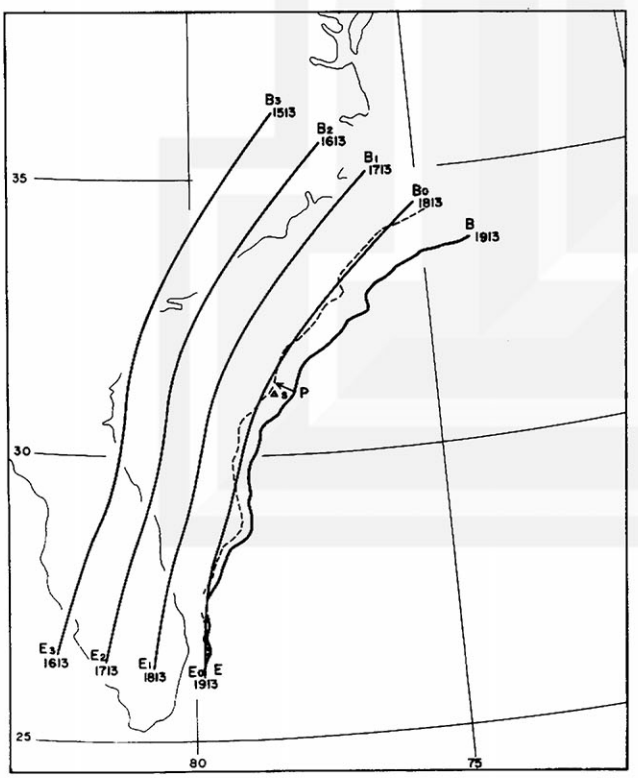

Fig. 8. Locations of possible flight paths (smooth solid lines) by projecting along the average wind. First approximation to the flight path along which the contrail was produced (dashed line).

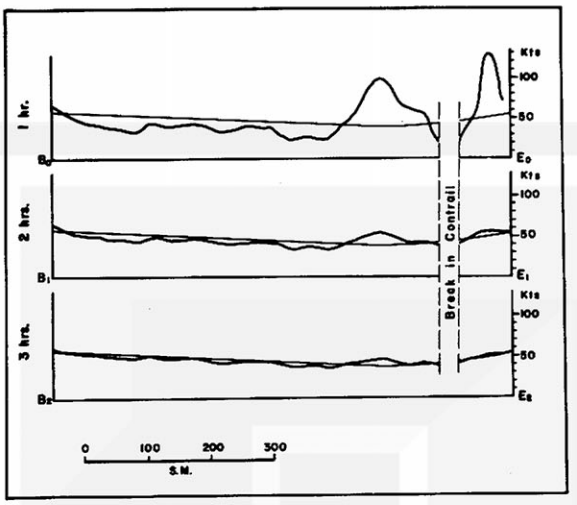

Fig. 9. Comparisons of the profile of the average wind determined from the meteorological data with the wind profile computed from the displacements of the contrail from an assumed smooth path along the indicated flight paths.

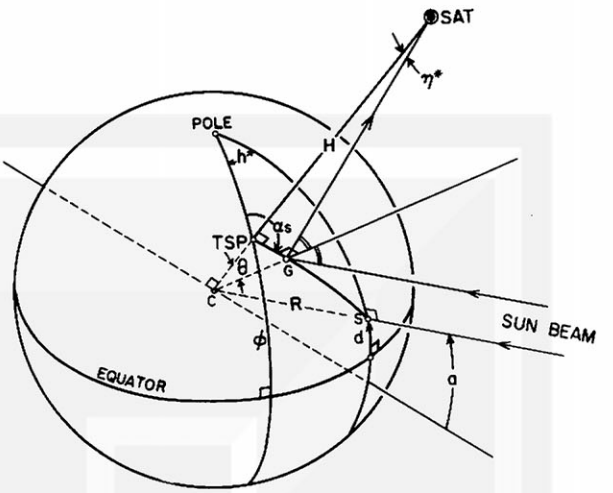

Fig. 10. Perspective view of the geometry in the Earth satellite system. C is the center of the Earth; G is the position on the Earth of the sun glint. S is the point of intersection of the sunbeam drawn to the center of the Earth, normal at the Earth's surface.

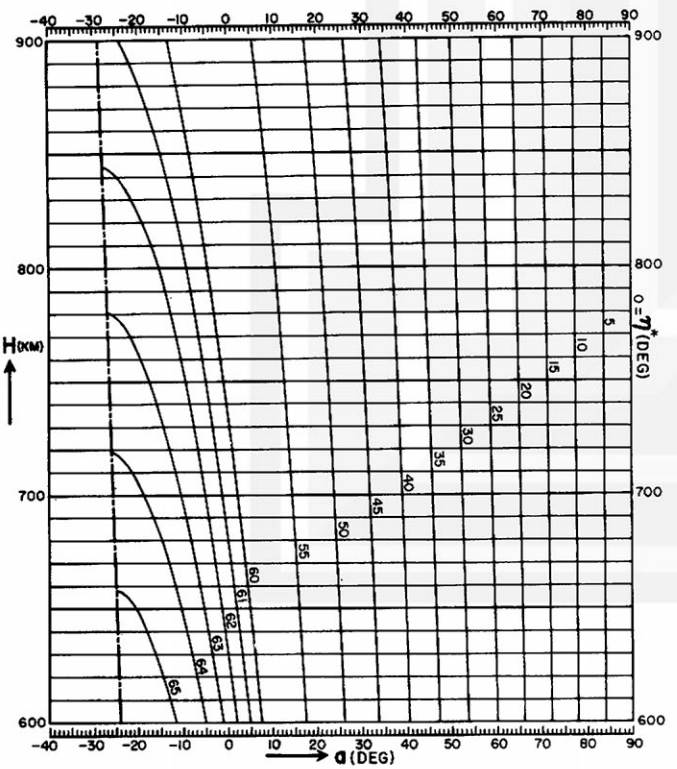

Fig. 11. Nomogram for the computation of the object-nadir angle (η^*) of the sun glint.

MESOMETEOROLOGY PROJECT ---- RESEARCH PAPERS

1. Report on the Chicago Tornado of March 4, 1961 - Rodger A. Brown and Tetsuya Fujita

2. Index to the NSSP Surface Network - Tetsuya Fujita

3. Outline of a Technique for Precise Rectification of Satellite Cloud Photographs - Tetsuya Fujita

4. Horizontal Structure of Mountain Winds - Henry A. Brown

5. An Investigation of Developmental Processes of the Wake Depression Through Excess Pressure Analysis of Nocturnal Showers - Joseph L. Goldman

6. Precipitation in the 1960 Flagstaff Mesometeorological Network - Kenneth A. Styber

7. On a Method of Single- and Dual-Image Photogrammetry of Panoramic Aerial Photographs - Tetsuya Fujita

8. A Review of Researches on Analytical Mesometeorology - Tetsuya Fujita

9. Meteorological Interpretations of Convective Nephsystems Appearing in TIROS Cloud Photographs - Tetsuya Fujita, Toshimitsu Ushijima, William A. Hass, George T. Dellert, Jr.

10. Study of the Development of Prefrontal Squall-Systems Using NSSP Network Data- Joseph L. Goldman

11. Analysis of Selected Aircraft Data from NSSP Operation, 1962 - Tetsuya Fujita